Catalysis by Ribonuclease A Is Limited by the Rate of Substrate Association†

Chiwook Park‡,§ and Ronald T. Raines*,‡,||

Department of Biochemistry and Department of Chemistry, University of Wisconsin−Madison, Madison, Wisconsin 53706

Received May 6, 2002; Revised Manuscript Received January 28, 2003

ABSTRACT: The value of k_{cat}/K_M for catalysis of RNA cleavage by ribonuclease (RNase) A can exceed 10^9 M^{-1} s^{-1} in a solution of low salt concentration. This value approaches that expected for the diffusional encounter of the enzyme and its substrate. To reveal the physicochemical constraints upon catalysis by RNase A, the effects of salt concentration, pH, solvent isotope, and solvent viscosity on catalysis were determined with synthetic substrates that bind to all of the enzymic subsites and thereby enable a meaningful analysis. The pK_a values determined from pH−k_{cat}/K_M profiles at 0.010, 0.20, and 1.0 M NaCl are inconsistent with the known macroscopic pK_a values of RNase A. This incongruity indicates that catalysis of RNA cleavage by RNase A is limited by the rate of substrate association, even at 1.0 M NaCl. The effect of solvent isotope and solvent viscosity on catalysis support this conclusion. The data are consistent with a mechanism in which RNase A associates with RNA in an intermediate complex, which is stabilized by Coulombic interactions, prior to the formation of a Michaelis complex. Thus, RNase A has evolved to become an enzyme limited by physics rather than chemistry, a requisite attribute of a perfect catalyst.

Enzymes catalyze specific reactions with enormous rate enhancement (*1*) and can even evolve to become perfect catalysts (*2*). Catalysis by a perfect enzyme is not limited by the rate of the chemical transformation of substrate to product. Rather, catalysis is limited by the rate of a physical step—substrate association or product dissociation. Such a consummation is achieved by optimizing the affinity of an enzyme for intermediates and transition states in its reaction pathway (*3*, *4*).

The rate of substrate association to form a Michaelis complex is not necessarily equal to the rate of physical encounter. The active site of an enzyme occupies only a small fraction of its surface (*5*). In addition, substrate association requires that the active-site residues and substrate assume a specific conformation and relative orientation (*6*). Thus, to bring catalysis to the encounter limit, an enzyme must develop tactics to accelerate substrate association as well as the chemical transformation.

Ribonuclease A (RNase A[1]; EC 3.1.27.5) was perhaps the most studied enzyme of the 20th century (*7*). Studies on the energetics of cleavage of UpA by RNase A have shown that k_{cat}/K_M for the cleavage of this small substrate is limited by substrate desolvation and that k_{cat} is partially limited by product release (*8*, *9*). RNase A has a series of phosphoryl group-binding subsites beyond its active site (*10*−*16*). These subsites, which are cationic, contribute significantly to catalysis via favorable Coulombic interactions with the phosphoryl groups of an RNA substrate, which are anionic (*14*, *17*, *18*). Recently, we described a synthetic DNA−RNA chimeric substrate, 6-carboxyfluorescein∼dArU$(dA)_2$∼6-carboxytetramethylrhodamine (6-FAM∼dArU$(dA)_2$∼6-TAMRA), that can occupy all of the subsites of RNase A but has only one scissile bond (*19*, *20*). The value of k_{cat}/K_M (3.6×10^7 M^{-1} s^{-1}; 0.10 M MES-NaOH buffer, pH 6.0, containing 0.10 M NaCl) for the cleavage of this optimized substrate is greater than those determined likewise for other substrates, like UpA (2.3×10^6 M^{-1} s^{-1}) and poly(C) (1.5×10^7 M^{-1} s^{-1}) (*21*). Moreover, the value of k_{cat}/K_M was determined to be $(2.7 \pm 0.5) \times 10^9$ M^{-1} s^{-1} at low salt concentration (1.0 mM Bistris-HCl buffer, pH 6.0, containing 0.010 M NaCl) (*21*).

The high value of k_{cat}/K_M for RNase A indicates that the mere encounter of the enzyme and substrate could limit catalysis (*22*), at least at low salt concentration. For example, Ca^{2+} and $(Lys)_3$ have been reported to associate with $A(pA)_4$ with bimolecular rate constants of 4.6×10^{10} M^{-1} s^{-1} (*23*) and 1.4×10^{10} M^{-1} s^{-1} (*24*), respectively, at low salt (1 mM sodium cacodylate). The diffusion coefficient of Ca^{2+} ion is 7.92×10^{-6} cm^2 s^{-1} at 25 °C (*25*), which is 6-fold greater than the diffusion coefficient of RNase A, 1.19×10^{-6} cm^2 s^{-1} at 20 °C (*26*). Hence, the k_{cat}/K_M of RNase A at 0.010 M NaCl is indeed comparable to that expected for an encounter-controlled reaction. This finding has inspired us to revisit the energetics of catalysis by RNase A.

Here, the effects of salt concentration, pH, solvent isotope, and solvent viscosity on catalysis by RNase A are determined

† This work was supported by Grants GM44783 and CA73808 (NIH).

* To whom correspondence should be addressed. Telephone: (608) 262-8588. Fax: (608) 262-3453. E-mail: Raines@biochem.wisc.edu.

‡ Department of Biochemistry.

§ Present address: Department of Molecular and Cell Biology, University of California, Berkeley, 229 Stanley Hall, Berkeley, CA 94720.

|| Department of Chemistry.

[1] Abbreviations: 4-DABCYL, 4-((4-(dimethylamino)phenyl)azo)-benzoic acid; 6-FAM, 6-carboxyfluorescein; 6-TAMRA, 6-carboxytetramethylrhodamine; Bistris, [bis(2-hydroxyethyl)amino]tris(hydroxymethyl)methane; cCMP, cytidine 2′,3′-cyclic phosphate; CpA, cytidylyl(3′→5′)adenosine; cUMP, uridine 2′,3′-cyclic phosphate; MES, 2-morpholinoethanesulfonic acid; NMR, nuclear magnetic resonance; poly(C), poly(cytidylic acid); RNase A, bovine pancreatic ribonuclease A; UpA, uridylyl(3′→5′)adenosine; UpU, uridylyl(3′→5′)uridine.

10.1021/bi026076k CCC: $25.00
Published on Web 03/04/2003

with our optimized substrate. The data reveal that catalysis is indeed limited by encounter at low salt concentration. Moreover, substrate association, not chemical transformation, limits catalysis, even at 1.0 M NaCl. From this comprehensive new information on the energetics of catalysis by RNase A, a model is proposed to explain how the enzyme associates with its substrate at the rate of encounter.

MATERIALS AND METHODS

Materials. Wild-type RNase A and its H12A variant were produced, folded, and purified as described elsewhere (*27*, *28*). UpA was a generous gift of J. E. Thompson. 6-FAM∼dArU(dA)$_2$∼4-DABCYL and 6-FAM∼dArU(dA)$_2$∼6-TAMRA were from Integrated DNA Technologies (Coralville, IA) (*19*, *20*).

[Bis(2-hydroxyethyl)amino]tris(hydroxymethyl)methane (Bistris) was from ICN Biomedicals (Aurora, OH). 2-(*N*-Morpholino)ethanesulfonic acid (MES) was from Sigma Chemical (St. Louis, MO). NaCl was from Fisher Scientific (Fair Lawn, NJ). D_2O was from Cambridge Isotope Laboratories (Andover, MA).

Concentrations of wild-type RNase A and its variants were determined by ultraviolet spectroscopy using $\epsilon = 0.72$ mL mg^{-1} cm^{-1} at 277.5 nm (*29*). The concentration of UpA was determined by ultraviolet spectroscopy using $\epsilon = 24\,600$ M^{-1} cm^{-1} at 260 nm at pH 7.0. Concentrations of 6-FAM∼dArU(dA)$_2$∼4-DABCYL and 6-FAM∼dArU(dA)$_2$∼6-TAMRA were determined by ultraviolet spectroscopy using $\epsilon = 77\,180$ and $102\,400$ M^{-1} cm^{-1}, respectively, at 260 nm.

Assays of Enzymatic Catalysis. The catalytic activity of RNase A was determined by monitoring the change in fluorescence intensity upon the cleavage of the two fluorogenic substrates (*19*, *20*). Assays were performed at 23 °C with stirring in 2.00 mL of buffer containing NaCl (0.010−1.0 M), H12A RNase A (5.0 nM), the fluorogenic substrates, and RNase A. H12A RNase A was added to reaction mixtures to absorb any possible inhibitory contaminants from buffer solutions (*30*). The catalytic contribution of 5.0 nM H12A RNase A was negligible herein because of its low catalytic activity (*31*, *32*). Fluorescence was measured with a QuantaMaster 1 photon-counting fluorescence spectrometer from Photon Technology International (South Brunswick, NJ), using 493 and 515 nm as excitation and emission wavelengths, respectively. Values of k_{cat}/K_M were determined from the change in fluorescence intensity, as described previously (*19*, *20*).

pH−k_{cat}/K_M Profiles. The effect of pH on the value of k_{cat}/K_M for the cleavage of 6-FAM∼dArU(dA)$_2$∼4-DABCYL by wild-type RNase A was determined in 2.00 mL of 1.0 mM buffer containing NaCl (0.010−1.0 M), H12A RNase A (5.0 nM), 6-FAM∼dArU(dA)$_2$∼4-DABCYL, and wild-type RNase A (5.0 pM to 0.50 nM). Buffers were sodium formate-HCl (pH 3.54−4.23), sodium acetate-HCl (pH 4.37−5.61), Bistris-NaOH (pH 5.87−6.66), MOPS-NaOH (pH 6.93−7.48), and Tris-HCl (pH 7.85−8.71). The pH values of buffers were determined with a Φ40 pH meter from Beckman instruments (Fullerton, CA). The pH values of reaction mixtures did not vary, even after complete cleavage of the substrates by RNase A. Salt effects on RNase A catalysis are mainly the result of specific interactions of cations with anionic RNA (*14*, *21*), and a constant ionic strength does not guarantee an identical salt environment. Hence, buffer concentration was kept low (1.0 mM) to provide a nearly identical salt environment at different pH values. 6-FAM∼dArU(dA)$_2$∼4-DABCYL rather than 6-FAM∼dArU(dA)$_2$∼6-TAMRA was used because the chemical stability of 4-DABCYL is greater than that of 6-TAMRA at acidic pH. Higher concentrations of the substrate were used at acidic pH (24−47 nM) than at basic pH (12 nM) because protonation of the fluorescein moiety of the substrate decreases its fluorescence intensity at acidic pH (*33*).[2] Nonlinear regression with the program SIGMAPLOT 5.0 (SPSS; Chicago, IL) was used to fit pH−k_{cat}/K_M profiles to eq 1:

$$k_{cat}/K_M = \frac{(k_{cat}/K_M)_{MAX}}{\frac{[H^+]}{K_1} + 1 + \frac{K_2}{[H^+]}} \quad (1)$$

where K_1 and K_2 are apparent macroscopic acid dissociation constants.

Solvent Isotope Effects. The effect of solvent isotope on k_{cat}/K_M for the cleavage of 6-FAM∼dArU(dA)$_2$∼6-TAMRA by wild-type RNase A (0.050 nM) was determined in 1.0 mM Bistris buffer containing NaCl (0.010−1.0 M) and H12A RNase A (5.0 nM). To minimize the difference in the ionization states of the active-site histidine residues in the H_2O and D_2O buffers, k_{cat}/K_M values in D_2O were determined in 1.0 mM Bistris-DCl buffer prepared by diluting 0.10 M Bistris-HCl buffer (pH 6.0) 100-fold with D_2O, assuming that the effect of solvent isotope on the pK_a values of the imidazolium group of a histidine residue is similar to that on the Bistris cation. For k_{cat}/K_M determination in D_2O, a solution of enzyme was prepared with D_2O buffer and incubated at least overnight at ambient temperature for complete isotope exchange of those functional groups that participate in catalysis. Further incubation of the enzyme in the D_2O buffer did not produce any detectable difference in cleavage rates. Solvent isotope effects were defined as the ratio of k_{cat}/K_M determined in H_2O to that determined in D_2O. Determination of solvent isotope effects was done in triplicate at each salt concentration.

Solvent isotope effects on the transphosphorylation reaction catalyzed by RNase A were also studied with a dinucleotide substrate, UpA. Cleavage of UpA was monitored by following the decrease in absorbance at 286 nm by ultraviolet spectroscopy ($\Delta\epsilon = -620$ M^{-1} cm^{-1} (*35*)). Assays were performed in 0.10 M MES-NaOH buffer (pH 6.0 or pD 6.4) containing NaCl (0.10 M), wild-type RNase A (0.20 nM in H_2O and 1.0 nM in D_2O), and UpA (0.074−1.1 mM). The pD value of the D_2O buffer was calculated by adding 0.4 to the pH meter reading (*36*). Kinetic parameters were determined by fitting the observed reaction rates to the Michaelis−Menten equation (*37*) by nonlinear regression.

Viscosity Effects. The effects of medium viscosity on k_{cat}/K_M for the cleavage of 6-FAM∼dArU(dA)$_2$∼6-TAMRA by RNase A were determined in 1.0 mM Bistris buffer (pH 6.0) containing sucrose (34.0% w/v), NaCl (0.10 or 1.0 M), wild-

[2] The pK_a of fluorescein in water is 6.5 (*34*).

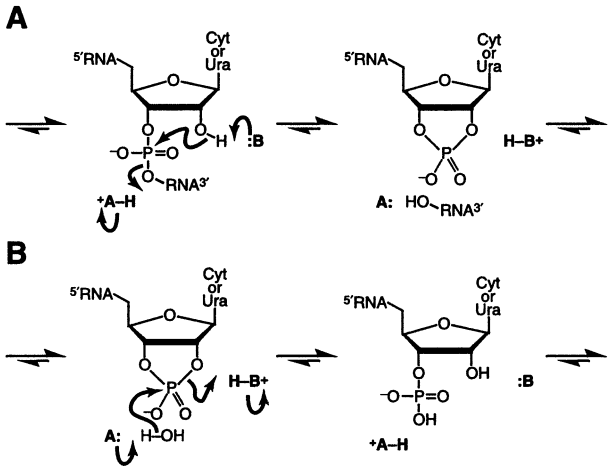

FIGURE 1: Putative mechanism of catalysis by ribonuclease A (*38*, *39*). (A) Transphosphorylation reaction. (B) Hydrolysis reaction. In both reactions, **B** and **A** refer to His12 and His119, respectively.

type RNase A (0.050 nM), and H12A RNase A (5.0 nM). Viscosity (η) was determined as the product of the kinematic viscosity (η/ρ) measured with an Ostwald viscometer at 23 °C and the density (ρ) of each solution, which was determined by weighing a known volume (Table 4). Relative viscosity ($\eta/\eta°$) refers to the ratio of the viscosity of a solution with sucrose to that of the same solution without sucrose. A medium viscosity effect was defined as the ratio of k_{cat}/K_M determined without sucrose to the k_{cat}/K_M determined with sucrose. Determination of medium viscosity effects was done in triplicate at each salt concentration. The viscosity effect at 0.010 M NaCl was indeterminable because of strong inhibition by a contaminant in low-salt solutions of commercial sucrose.

RESULTS

Effect of pH on Catalysis by RNase A. RNase A cleaves RNA molecules by concerted general acid−base catalysis using the active-site residues His12 and His119 (Figure 1) (*31*, *38*−*41*). The need for both a protonated and an unprotonated histidine residue for efficient catalysis results in bell-shaped pH−k_{cat}/K_M profiles with two pK_a values near 6 for the cleavage of dinucleotides and hydrolysis of nucleotide 2′,3′-cyclic phosphates (*38*, *42*, *43*). The pK_a values from these pH−k_{cat}/K_M profiles are consistent with the microscopic pK_a values of the active-site histidine residues determined by NMR spectroscopy (*44*).

Here, the values of k_{cat}/K_M for the cleavage of 6-FAM∼dArU(dA)$_2$∼4-DABCYL by RNase A were determined at varying pH at three different salt concentrations (Figure 2 and Table S1 in Supporting Information). Parameters determined by fitting the data to eq 1 are listed in Table 1.

The pH−k_{cat}/K_M profile at 0.010 M NaCl has a wide plateau with pK_a values of 3.88 ± 0.06 and 7.47 ± 0.06. The $(k_{cat}/K_M)_{MAX}$ is (2.8 ± 0.1) × 10^9 M^{-1} s^{-1}. Because of the lack of data at low and high pH, the uncertainty in these pK_a values could exceed the standard errors from the nonlinear regression.

The pH−k_{cat}/K_M profile at 0.20 M NaCl has a more narrow plateau than does that determined at 0.010 M NaCl. The values of pK_a and $(k_{cat}/K_M)_{MAX}$ are 4.66 ± 0.09 and 6.44 ± 0.08, and (6.7 ± 0.9) × 10^7 M^{-1} s^{-1}. The profile has an asymmetric bell shape, and the slope of the acidic arm

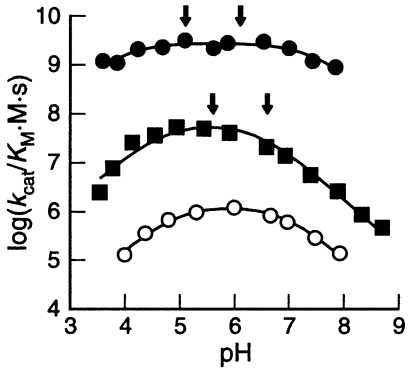

FIGURE 2: pH−k_{cat}/K_M profiles for the cleavage of 6-FAM∼dArU(dA)$_2$∼4-DABCYL by ribonuclease A at 0.010 (●), 0.20 (■), and 1.0 M (○) NaCl. The assays were performed at 23 °C in 1.0 mM buffer containing NaCl. Determination of k_{cat}/K_M values at each pH was done in triplicate (Table S1 in Supporting Information). Each curve was fitted to eq 1 by nonlinear regression. Values of apparent pK_a and $(k_{cat}/K_M)_{MAX}$ are listed in Table 1. Arrows indicate macroscopic pK_a values of ribonuclease A determined by NMR spectroscopy under similar conditions (0.018 and 0.142 M NaCl without buffer (*48*)).

Table 1: Parameters[a] Determined from the pH Dependence of k_{cat}/K_M for the Cleavage of 6-FAM∼dArU(dA)$_2$∼4-DABCYL by Ribonuclease A at 0.010, 0.20, and 1.0 M NaCl

[NaCl] (M)	pK_1	pK_2	$(k_{cat}/K_M)_{MAX}$ (M^{-1} s^{-1})
0.010	3.88 ± 0.06 (5.1[b])	7.47 ± 0.06 (6.1[b])	(2.8 ± 0.1) × 10^9
0.20	4.66 ± 0.09 (5.6[b])	6.44 ± 0.08 (6.6[b])	(6.7 ± 0.9) × 10^7
1.0	4.88 ± 0.04	6.95 ± 0.04	(1.4 ± 0.1) × 10^6

[a] Values (±SE) were determined by fitting the data in Figure 2 to eq 1 by nonlinear regression. [b] Macroscopic pK_a values of ribonuclease A calculated from microscopic pK_a values of His12 and His119 determined by NMR spectroscopy under similar conditions (0.018 and 0.142 M NaCl without buffer) (*48*).

appears to be greater than that of the basic arm. This greater slope indicates that two titratable groups affect catalysis below pH 4.0. The additional titration near pH 4 has also been observed in both pH-rate profiles determined with uridine 2′,3′-cyclic phosphate (cUMP) (*45*) and the titration of His12 by NMR spectroscopy (*46*). Although the use of an equation with two basic functional groups and one acidic functional group improved the fitting to the profile (data not shown), the nonlinear regression did not produce statistically meaningful pK_a values for both basic groups. Thus, only pK_a values determined by fitting the profile to eq 1 are listed in Table 1.

The pH−k_{cat}/K_M profile at 1.0 M NaCl has a symmetric bell shape. The pK_a and $(k_{cat}/K_M)_{MAX}$ values are 4.88 ± 0.04 and 6.95 ± 0.04, and (1.4 ± 0.1) × 10^6 M^{-1} s^{-1}. These pK_a values are greater than those determined at 0.20 M NaCl.

The pK_a values determined from the pH−k_{cat}/K_M profiles do not agree with the macroscopic pK_a values of RNase A. The macroscopic pK_a values of an enzyme can be calculated from the microscopic pK_a values of its catalytically significant titratable groups (*47*). The microscopic pK_a values of the active-site histidine residues determined by NMR spectroscopy (*48*) were used to estimate the macroscopic pK_a values of RNase A (Table 1). These macroscopic pK_a values are 5.1 and 6.1 at 0.018 M NaCl. At a similar concentration of NaCl (0.010 M), the pH−k_{cat}/K_M profile for the cleavage

Table 2: Solvent Isotope Effects on the Cleavage of 6-FAM∼dArU(dA)$_2$∼6-TAMRA by Ribonuclease A at 0.010, 0.20, and 1.0 M NaCl[a]

[NaCl] (M)	$^{D_2O}(k_{cat}/K_M)$[b]
0.010	1.18 ± 0.05
0.10	1.40 ± 0.15
1.0	1.76 ± 0.02

[a] Assays were performed at 23 °C in 1.0 mM Bistris-HCl buffer (pH 6.0) containing NaCl in H_2O and D_2O. [b] $^{D_2O}k_{cat}/K_M$ is defined as the ratio of $(k_{cat}/K_M)^{H_2O}$ to $(k_{cat}/K_M)^{D_2O}$. Errors are standard deviations of triplicate determinations.

Table 3: Solvent Isotope Effects on the Cleavage of UpA by Ribonuclease A[a]

solvent	k_{cat}/K_M (10^6 M^{-1} s^{-1})	k_{cat} (10^3 s^{-1})
H_2O	3.5 ± 0.3	2.9 ± 0.3
D_2O	0.89 ± 0.04	1.8 ± 0.2
isotope effects[b]	3.9 ± 0.4	1.6 ± 0.2

[a] Assays were performed at 25 °C in 0.10 M MES-NaOH (pH 6.0 or pD 6.4) containing NaCl (0.10 M) in H_2O and D_2O. [b] Isotope effects are defined as the ratio of kinetic parameters determined in H_2O to those determined in D_2O.

of 6-FAM∼dArU(dA)$_2$∼4-DABCYL by RNase A shows pK_a values of 3.88 ± 0.06 and 7.47 ± 0.06 (Table 1). Although these pK_a values have some statistical uncertainty because of the lack of data at low and high pH (Figure 2), these values are certainly distinct from the macroscopic pK_a values of RNase A. At 0.142 M NaCl, the macroscopic pK_a values of RNase A are increased to 5.6 and 6.6. The pH−k_{cat}/K_M profile determined at 0.20 M NaCl shows pK_a values of 4.66 ± 0.09 and 6.44 ± 0.08 (Table 1). Whereas the pK_2 from the pH−k_{cat}/K_M profile (6.44 ± 0.08) is close to the macroscopic pK_2 (6.6), the pK_1 from the pH−k_{cat}/K_M profile (4.66 ± 0.09) is distinct from the macroscopic pK_2 (5.6). The microscopic pK_a values of the histidine residues at 1.0 M are not known. From the effect of increasing NaCl concentration from 0.018 to 0.142 M on the macroscopic pK_a values, the pK_a values at 1.0 M NaCl are expected to be higher by 0.4−0.5 unit than the pK_a values determined at 0.142 M NaCl. The pH−k_{cat}/K_M profile determined at 1.0 M NaCl shows pK_a values of 4.88 ± 0.04 and 6.95 ± 0.04 (Table 1). The pK_2 value seems to be consistent with the macroscopic pK_2 value, considering the expected increase from an increase in salt concentration. The pK_1 value, however, is still not consistent with the macroscopic pK_1 of RNase A.

Solvent Isotope Effects. Solvent isotope effects on k_{cat}/K_M for the cleavage of 6-FAM∼dArU(dA)$_2$∼6-TAMRA by RNase A were determined at three different salt concentrations (Table 2). The $^{D_2O}(k_{cat}/K_M)$ values are 1.18 ± 0.05, 1.40 ± 0.15, and 1.76 ± 0.02 at 0.010, 0.10, and 1.0 M NaCl, respectively.

Solvent isotope effects on the value of k_{cat}/K_M and k_{cat} for the cleavage of UpA by RNase A were also determined for comparison (Table 3). At 0.142 M NaCl, $^{D_2O}(k_{cat}/K_M)$ was determined to be 3.9 ± 0.4, which is much greater than any of the $^{D_2O}(k_{cat}/K_M)$ values determined with 6-FAM∼dArU(dA)$_2$∼6-TAMRA (Table 2). The value of $^{D_2O}k_{cat}$ was determined to be 1.6 ± 0.2 with UpA (Table 3).

Viscosity Effects. The viscogen sucrose was used to probe the contribution of the rate of substrate association to k_{cat}/K_M (Table 4). Viscosity effects of 34.0% (w/v) sucrose on k_{cat}/K_M for the cleavage of 6-FAM∼dArU(dA)$_2$∼6-TAMRA were determined to be 3.2 ± 0.1 and 3.4 ± 0.2 at 0.10 and 1.0 M NaCl, respectively. The viscosity effects are close to the relative viscosity of the solution at each salt concentration (Table 4).

Table 4: Medium Viscosity Effects on the Cleavage of 6-FAM∼dArU(dA)$_2$∼6-TAMRA by Ribonuclease A at 0.10 and 1.0 M NaCl[a]

[NaCl] (M)	density[b]	concentration[c] (% w/w)	relative visc. ($\eta/\eta°$)[d]	visc. effect[e]
0.10	1.125 ± 0.002	30.2 ± 0.1	3.10 ± 0.02	3.2 ± 0.1
1.0	1.168 ± 0.001	29.1 ± 0.1	3.31 ± 0.02	3.4 ± 0.2

[a] Assays were performed at 23 °C in 1.0 mM Bistris-HCl buffer (pH 6.0) containing NaCl with or without sucrose (34% w/v). [b] Density (±SE) of the solution was determined by weighing. [c] Concentration (±SE) was determined by dividing 34% (w/v) by the density of the solution. [d] Relative viscosity (±SE) was determined as a product of the kinematic viscosity (η/ρ) measured at 23 °C and the density (ρ) of each solution. [e] Viscosity effect is defined as the ratio of k_{cat}/K_M determined without sucrose to that determined with 34% (w/v) sucrose.

DISCUSSION

Deduction of pK_a Values from pH−k_{cat}/K_M Profiles. An apparent pK_a value determined from the pH−k_{cat}/K_M profile of an enzyme-catalyzed reaction is often interpreted to be the macroscopic pK_a value of a catalytically significant titratable group of the free enzyme (*49*, *50*). Such pK_a values are independent of the substrate used to determine k_{cat}/K_M values, as shown in pH−k_{cat}/K_M profiles for the RNase A-catalyzed transphosphorylation of UpA, UpU, and CpA (*51*) and hydrolysis of cytidine 2′,3′-cyclic phosphate (cCMP) (*42*, *52*) and cUMP (*43*, *45*). The notion that pH−k_{cat}/K_M profiles manifest macroscopic pK_a values of an enzyme is, however, based on the assumption that the substrate is not sticky.[3] If this assumption is incorrect, then the pH−k_{cat}/K_M profile could depict mirage pK_a values (*49*, *50*), which do not reflect the actual acid dissociation constants of the enzyme. Indeed, the pH−k_{cat}/K_M profiles for the cleavage of 6-FAM∼dArU(dA)$_2$∼4-DABCYL by RNase A (Figure 2) do not reflect the macroscopic pK_a values of RNase A (Table 1). These inconsistencies between the pK_a values from pH−k_{cat}/K_M profiles and the macroscopic pK_a values of RNase A are consistent with 6-FAM∼dArU(dA)$_2$∼4-DABCYL being a sticky substrate that undergoes rapid cleavage after it forms a Michaelis complex with RNase A.

Analysis of pH−k_{cat}/K_M Profiles. A kinetic mechanism for catalysis of RNA cleavage by RNase A is depicted in Figure 3A. The macroscopic acid dissociation constants of the free enzyme are K_1 and K_2. The second-order rate constants for the substrate-association steps are k_1, k_1', and k_1''; the first-order rate constants for the substrate-dissociation steps are k_2, k_2', and k_2''. The rate constant for the chemistry step is k_3.[4]

The equation describing the pH−k_{cat}/K_M profile for the kinetic mechanism in Figure 3A includes 11 rate constants and two acid dissociation constants:

[3] A sticky substrate is one in which the initial enzyme−substrate encounter complex proceeds through the first irreversible step (such as the release of the first product) faster than it releases unreacted substrate (*53*).

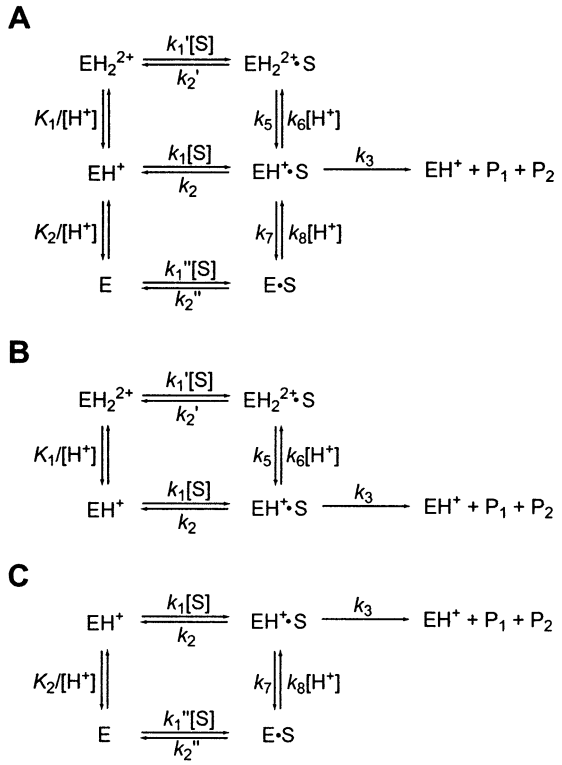

FIGURE 3: Kinetic mechanisms of catalysis by ribonuclease A. (A) The kinetic mechanism with parallel pathways that lead to a Michaelis complex, $EH^+\bullet S$. K_1 and K_2 are equilibrium acid dissociation constants of the free enzyme; k_5, k_6, k_7, and k_8 are acid dissociation rate constants of the ES complex. k_1, k_1', and k_1'' are rate constants of substrate-association steps; k_2, k_2', and k_2'' are rate constants of substrate-dissociation steps. k_3 is the rate constant of the chemistry step. (B) The kinetic mechanism for the acidic titration with pK_1. (C) The kinetic mechanism for the basic titration with pK_2.

$$k_{cat}/K_M = \frac{\left(\frac{k_1' k_5}{k_2' + k_5}\frac{[H^+]}{K_1} + k_1 + \frac{k_1'' k_8[H^+]}{k_2'' + k_8[H^+]}\frac{K_2}{[H^+]}\right)k_3}{\left(\frac{[H^+]}{K_1} + 1 + \frac{K_2}{[H^+]}\right)\left(\frac{k_2' k_6[H^+]}{k_2' + k_5} + k_2 + k_3 + \frac{k_2'' k_7}{k_2'' + k_8[H^+]}\right)} \quad (2)$$

This equation is impractical to use for fitting pH$-k_{cat}/K_M$ profiles.[5] The pH$-k_{cat}/K_M$ profile can be analyzed, however, by considering the acidic titration (K_1) and the basic titration (K_2) separately.

The mechanism in Figure 3B depicts the acidic titration with pK_1. The equation that describes the pH$-k_{cat}/K_M$ profile of this mechanism can be expressed as

$$k_{cat}/K_M = \frac{\left(1 + \frac{[H^+]}{K_\alpha}\right)\left(\frac{k_1 k_3}{k_2 + k_3}\right)}{\left(1 + \frac{[H^+]}{K_1}\right)\left(1 + \frac{[H^+]}{\sigma K_\alpha}\right)} \quad (4)$$

where

$$K_\alpha = \left(\frac{k_1}{k_1'}\right)\left(1 + \frac{k_2'}{k_5}\right)K_1 \quad (5)$$

and

$$\sigma = \left(1 + \frac{k_3}{k_2}\right) = 1 + S_r \quad (6)$$

S_r is a stickiness ratio (*55*), which herein is the ratio of k_3 to k_2. When the substrate is not sticky, $S_r = 0$ and eq 4 simplifies to the familiar form

$$k_{cat}/K_M = \frac{\frac{k_1 k_3}{k_2 + k_3}}{1 + \frac{[H^+]}{K_1}} = \frac{(k_{cat}/K_M)_{MAX}}{1 + \frac{[H^+]}{K_1}} \quad (7)$$

Accordingly, the pH$-k_{cat}/K_M$ profile manifests K_1, the actual macroscopic pK_a value of the enzyme, if the substrate is not sticky. pH$-k_{cat}/K_M$ profiles determined for the turnover of UpA and cCMP by RNase A manisfest this case.

If the substrate is sticky, however, the apparent pK_a from the pH$-k_{cat}/K_M$ profile is dependent on the magnitudes of σ and K_α in eq 4. The pH$-k_{cat}/K_M$ profiles determined with 6-FAM~dArU(dA)$_2$~4-DABCYL at 0.010, 0.20, and 1.0 M NaCl (Figure 2) show shifted pK_a values and plateaus, which indicates that $K_\alpha = K_1$. (If $K_\alpha \neq K_1$, then the profiles would have a hump or hollow rather than a plateau (*53*).) From eq 5, K_α is equal to K_1 if EH_2^{2+} and EH^+ associate with the substrate at the same rate ($k_1 = k_1'$) and proton release is much faster than substrate release from $EH_2^{2+}\bullet S$ ($k_5 \gg k_2'$). If $K_\alpha = K_1$, then eq 4 simplifies to

$$k_{cat}/K_M = \frac{\frac{k_1 k_3}{k_2 + k_3}}{1 + \frac{[H^+]}{\sigma K_1}} = \frac{(k_{cat}/K_M)_{MAX}}{1 + \frac{[H^+]}{\sigma K_1}} \quad (8)$$

and the apparent pK_a value from the pH$-k_{cat}/K_M$ profile differs from the actual macroscopic pK_a value by $-\log \sigma$:

$$pK_{apparent} = pK_1 - \log \sigma = pK_1 - \log(1 + S_r) \quad (9)$$

The apparent acidic pK_a values in the pH$-k_{cat}/K_M$ profiles determined at 0.010 and 0.20 M NaCl are shifted by 1.2

[4] If the kinetic mechanism in Figure 3A does not have parallel pathways (i.e., k_1', k_1'', k_2', and k_2'' are 0), then the pH$-k_{cat}/K_M$ profile would always portray the macroscopic acid dissociation constants, K_1 and K_2 (*47*, *49*). The abnormal pK_a values from the pH$-k_{cat}/K_M$ profiles indicate that the parallel pathways cannot be ignored.

[5] Acids and bases are not necessarily sequestered from solvent in the ES states. If $k_5 \gg k_2'$ and $k_8[H^+] \gg k_2''$ in Figure 3A (i.e., proton transfer in the ES states is faster than substrate release), then the effect of pH on k_{cat}/K_M can be described by eq 3 (*54*):

$$k_{cat}/K_M = \frac{\left(k_1'\frac{[H^+]}{K_1} + k_1 + k_1\frac{K_2}{[H^+]}\right)k_3}{\left(\frac{[H^+]}{K_1} + 1 + \frac{K_2}{[H^+]}\right)\left(k_2'\frac{[H^+]}{K_1'} + k_2 + k_3 + k_2\frac{K_2'}{[H^+]}\right)} \quad (3)$$

where $K_1' = k_5/k_6$ and $K_2' = k_7/k_8$. Eq 3, though simpler than eq 2, is still impractical to use for the fitting of experimental pH$-k_{cat}/K_M$ profiles.

and 0.9 units, respectively, from the macroscopic pK_a valueof RNase A (Table 1). From eq 9, the value of S_r is then 15 and 7 at 0.010 and 0.20 M NaCl, respectively. The apparent pK_a value determined at 1.0 M NaCl also seems to be distinct from the macroscopic pK_a value of the enzyme. Thus, the pH$-k_{cat}/K_M$ profiles indicate that the substrate is sticky ($S_r > 1$), even at 1.0 M NaCl.

The mechanism in Figure 3C depicts the basic titration with pK_2. The equation that describes the pH$-k_{cat}/K_M$ profile of this mechanism can be expressed as

$$k_{cat}/K_M = \frac{\left(1 + \frac{K_\alpha}{[H^+]}\right)\left(\frac{k_1 k_3}{k_2 + k_3}\right)}{\left(1 + \frac{K_2}{[H^+]}\right)\left(1 + \frac{\sigma K_\alpha}{[H^+]}\right)} \quad (10)$$

where

$$K_\alpha = \left(\frac{k_1}{k_1}\right)\left(1 + \frac{k_2}{k_7}\right)K_2 \quad (11)$$

and

$$\sigma = \frac{\left(1 + \frac{k_3}{k_2 + k_7}\right)}{\left(1 + \frac{k_3}{k_2}\right)} \quad (12)$$

The pH$-k_{cat}/K_M$ profile determined at 0.010 M NaCl (Figure 2) shows a shifted pK_a value and plateau, which indicates that $K_\alpha = K_2$ in analogy to the acidic titration (vide supra). From eq 11, K_α is equal to K_2 if the substrate association rate for EH^+ and E are same ($k_1 = k_1''$) and proton release is much faster than substrate release from EH^+•S ($k_7 \gg k_2$). If $K_\alpha = K_2$, then the apparent pK_a value from the pH$-k_{cat}/K_M$ profile differs from the actual macroscopic pK_a value by $-\log \sigma$:

$$pK_{apparent} = pK_2 - \log \sigma = pK_2 + \log\left(\frac{1 + \frac{k_3}{k_2}}{1 + \frac{k_3}{k_2 + k_7}}\right) \quad (13)$$

The wide plateau with shifted pK_a values of the pH$-k_{cat}/K_M$ profile at 0.010 M NaCl is again indicative of a sticky substrate (*53*). The $(k_{cat}/K_M)_{MAX}$ value, $(2.8 \pm 0.1) \times 10^9$ M^{-1} s^{-1}, corresponds to the rate of substrate association, which is likely to be encounter-controlled. Moreover, the pH$-k_{cat}/K_M$ profile shows that the rate of substrate association is pH-independent at this salt concentration ($k_1 = k_1' = k_1''$).

The apparent basic pK_a values from the pH$-k_{cat}/K_M$ profiles at 0.20 and 1.0 M NaCl are close to the macroscopic pK_a values of RNase A (Table 1). Even when a substrate is sticky, the apparent pK_a of the pH$-k_{cat}/K_M$ profiles for the kinetic mechanism in Figure 3C can manifest the actual macroscopic pK_a value of an enzyme in two cases. First, if $\sigma = 1$ in eq 12, then the pH$-k_{cat}/K_M$ profile in eq 10 simplies to the familiar form

$$k_{cat}/K_M = \frac{\frac{k_1 k_3}{k_2 + k_3}}{1 + \frac{K_2}{[H^+]}} = \frac{(k_{cat}/K_M)_{MAX}}{1 + \frac{K_2}{[H^+]}} \quad (14)$$

For a sticky substrate ($k_3 \gg k_2$) to have $\sigma = 1$, proton release must be much slower than substrate release from EH^+•S ($k_7 \ll k_2$). Second, if $K_\alpha \ll K_2$, then the pH$-k_{cat}/K_M$ profile also simplifies to eq 14, which occurs when substrate associates much faster with EH^+ than with E ($k_1 \gg k_1''$). The data in Figure 2 are consistent with either of these cases. For example, the first case is possible if proton release from EH^+•S is hindered by the bound substrate, and the second case is possible if the cationic charges of active-site histidine residues have a role in facilitating substrate association. In either case, the pH$-k_{cat}/K_M$ profiles at 0.20 and 1.0 M NaCl are consistent with 6-FAM∼dArU$(dA)_2$∼4-DABCYL being a sticky substrate for RNase A.

Solvent Isotope Effect on Catalysis. The rate of the chemistry step during catalysis by RNase A (Figure 1) is sensitive to solvent isotope because protons are transferred in its transition state. Hence, the stickiness of a substrate can be assessed directly by measuring the solvent isotope effect. The solvent isotope effect on k_{cat}/K_M for RNase A can be written (*36*) as

$$^{D_2O}(k_{cat}/K_M) = \frac{(k_{cat}/K_M)^{H_2O}}{(k_{cat}/K_M)^{D_2O}} = \frac{^{D_2O}k_3 + C_f}{1 + C_f} \quad (15)$$

where $^{D_2O}k_3$ is the intrinsic isotope effect on the chemistry step and is defined as the ratio of k_3 in H_2O to k_3 in D_2O, and C_f is a forward commitment factor (*53*), which is the ratio of k_3 to k_2 when the medium is H_2O.[6]

The effect of solvent isotope on the cleavage of UpA by RNase A was determined and compared with that for the cleavage of 6-FAM∼dArU$(dA)_2$∼6-TAMRA. The value of $^{D_2O}(k_{cat}/K_M)$ for the cleavage of UpA by RNase A is 3.9 ± 0.4 (Table 3). This value is close to the solvent isotope effects on k_{cat}/K_M and k_{cat} for the hydrolysis of cCMP, which were determined previously to be ∼4 (*52*) and 3.1 (*56*), respectively. Because $C_f > 0$ in eq 2, the value of $^{D_2O}k_3$ is likely to be even greater than 3.9 ± 0.4. The value of $^{D_2O}k_{cat}$ for the cleavage of UpA by RNase A is 1.6 ± 0.2 (Table 3). Because $^{D_2O}k_{cat} < {}^{D_2O}k_3$, a step other than the chemistry step determines k_{cat}. This solvent isotope effect on k_{cat} is consistent with the observation that product release partially limits the value of k_{cat} for UpA cleavage by RNase A (*8*).

The solvent isotope effect on k_{cat}/K_M for the cleavage of 6-FAM∼dArU$(dA)_2$∼6-TAMRA by RNase A are much less than that for the cleavage of UpA (Table 2), which indicates that C_f is larger for the longer substrate. Because D_2O is more viscous than H_2O by a factor of 1.24 at 20 °C (*57*), solvent isotope effects from an increase in medium viscosity must be considered when C_f is large (*58*). Hence,

[6] In the general case, the stickiness ratio, S_r, is a function of several commitment factors, including C_f (*55*). Herein, C_f is identical to S_r.

eq 15 needs to be modified, as in eq 16:

$$^{D_2O}(k_{cat}/K_M) = \frac{^{D_2O}k_3 + 1.24C_f}{1 + C_f} \quad (16)$$

Thus, if a substrate is extremely sticky (i.e., $C_f \gg 1$), then $^{D_2O}(k_{cat}/K_M)$ would be close to 1.24 rather than unity. The solvent isotope effect of $^{D_2O}(k_{cat}/K_M) = 1.18 \pm 0.05$ at 0.010 M NaCl does indeed suggest an origin in the higher viscosity of D_2O and that k_{cat}/K_M is limited by substrate association. By assuming that $^{D_2O}k_3 = 3.9$ (as $^{D_2O}(k_{cat}/K_M) = (3.9 \pm 0.4)$ for the cleavage of UpA), eq 16 can be used to estimate that the value of C_f is 16 and 4 at 0.10 and 1.0 M NaCl, respectively, for the cleavage of 6-FAM∼dArU(dA)$_2$∼6-TAMRA by RNase A. These C_f values are in qualitative agreement with the values of S_r determined from pH−k_{cat}/K_M profiles (vide supra). Apparently, 6-FAM∼dArU(dA)$_2$∼6-TAMRA is indeed a sticky substrate, and substrate association limits k_{cat}/K_M, even at 1.0 M NaCl.

Medium viscosity effects corroborate this conclusion (Table 4). The frequency with which two molecules collide is inversely proportional to the microviscosity of the medium (*59*, *60*). Adding sucrose to 34% (w/v) both increases the medium viscosity and decreases the value of k_{cat}/K_M for the cleavage of 6-FAM∼dArU(dA)$_2$∼6-TAMRA by approximately 3-fold at 0.10 and 1.0 M NaCl (Table 4). Thus, the viscosity effects are consistent with the solvent isotope effects—substrate association limits k_{cat}/K_M for the cleavage of 6-FAM∼dArU(dA)$_2$∼6-TAMRA by RNase A, even at 1.0 M NaCl.

Salt Effect on Substrate Association. pH−k_{cat}/K_M profiles and solvent isotope effects show that k_{cat}/K_M for the cleavage for 6-FAM∼dArU(dA)$_2$∼4-DABCYL by RNase A is limited by the substrate-association rate at pH 6.0. Hence, the salt effect on k_{cat}/K_M actually reports on the salt effect on the substrate-association rate. The salt effect on k_{cat}/K_M for the cleavage of 6-FAM∼dArU(dA)$_2$∼6-TAMRA by RNase A has been analyzed quantitatively with eq 17 (*21*):

$$k_{cat}/K_M = \frac{(k_{cat}/K_M)_{MAX}}{1 + \left(\frac{[Na^+]}{K_{Na^+}}\right)^{n'}} \quad (17)$$

where $(k_{cat}/K_M)_{MAX}$ is the maximum of k_{cat}/K_M, n' is the absolute value of the slope in the linear region of a log[Na^+]−log(k_{cat}/K_M) plot, and K_{Na^+} is the salt concentration where k_{cat}/K_M is half of its maximum. The parameter n' is related to n, the number of Na^+ ions released from a substrate upon binding, as in eq 18:

$$\beta n < n' < n \quad (18)$$

where β is a correlation parameter for the salt effect on the free energy of the substrate-association transition state to that on the free energy of the ES state. When k_{cat}/K_M is limited completely by the chemistry step, $n' = n$. In the other extreme, when k_{cat}/K_M is limited completely by substrate association, $n' = \beta n$. The values of $(k_{cat}/K_M)_{MAX}$, n', and K_{Na^+} for the cleavage of 6-FAM∼dArU(dA)$_2$∼6-TAMRA by RNase A at pH 6.0 are $(3.3 \pm 0.4) \times 10^9$ M^{-1} s^{-1}, 2.33 ± 0.05, and (25 ± 2) mM, respectively (*21*). The value of $n' = 2.33 \pm 0.05$ is likely to correspond to βn because the cleavage of 6-FAM∼dArU(dA)$_2$∼4-DABCYL by RNase A is limited by the substrate-association rate at pH 6.0. The actual value of n is unknown but can be estimated from the salt effect on the k_{cat}/K_M value of K41R RNase A. Because K41R RNase A is a sluggish catalyst (*61*), the value of $n' = 2.66 \pm 0.08$ for K41R RNase A likely reflects n (*21*). By approximating n as 2.66, β is estimated to be ∼0.9 (*21*).

The observed effect of salt concentration on the solvent isotope effect is consistent with $\beta \approx 0.9$. The solvent isotope effect on cleavage of 6-FAM∼dArU(dA)$_2$∼6-TAMRA by RNase A does not vary significantly, even when the salt concentration is increased by 10^2-fold (Table 2). The forward commitment factor can be expressed as a function of [Na^+], as in eq 19 (*21*):

$$C_f = C_f^{\ominus}[Na^+]^{(\beta-1)n} \quad (19)$$

where $C_f^{\ominus}$ is the commitment factor when [Na^+] = 1.0 M. According to eq 19, when the value of β is close to 1, C_f (and hence the solvent isotope effect) is expected to be nearly independent of salt concentration.

The value of β reveals the nature of the transition state for the substrate-association step. If a Michaelis complex forms without an intermediate, then the salt effect on the association rate is expected to be minimal. For example, $\beta \approx 0.1$ for the single-step association of a protein and nucleic acid (*62*). The β value of ∼0.9 indicates that RNase A and its substrate form an intermediate during substrate association and that this intermediate contains almost as many Coulombic interactions as does the Michaelis complex.

Mechanism of Substrate Association by Ribonuclease A. To enhance the rate of association, biological systems use special tactics such as electrostatic guidance (*63*−*66*) and diffusion in reduced dimensions (*6*, *51*, *52*, *67*−*70*). Such precedents and the results reported here are consistent with a two-step mechanism for the binding of a substrate to RNase A (Figure 4). In this mechanism, RNase A diffuses to a substrate and forms a short-lived complex (E:S) through nonspecific Coulombic interactions between the substrate and the enzymic surface beyond the active site (*67*). The substrate then scans the surface of the enzyme by repeated inelastic collisions (*6*). If the substrate finds the active site of the enzyme before it dissociates from the enzyme, then the complex is stabilized by specific interactions between the active-site residues and the substrate (ES). Charged residues near the active site could steer the substrate to the active site (E:S → ES) by providing an appropriate electrostatic potential on the enzymic surface (*63*−*66*).

In solutions of high salt concentration, the free energies of E:S and the transition state between E:S and ES are so high that searching for the active site (E:S → ES) limits the substrate-association rate (Figure 4). The Coulombic nature of the transition state between E:S and ES gives the substrate-association rate its significant dependence on salt concentration ($\beta \approx 0.9$), as shown in the salt-rate profile (*21*). At 0.010 M NaCl, the transition state between E:S and ES is stabilized significantly, and the encounter of the enzyme and the substrate (E + S → E:S) determines the substrate-association rate, which is insensitive to salt concentration and pH, as

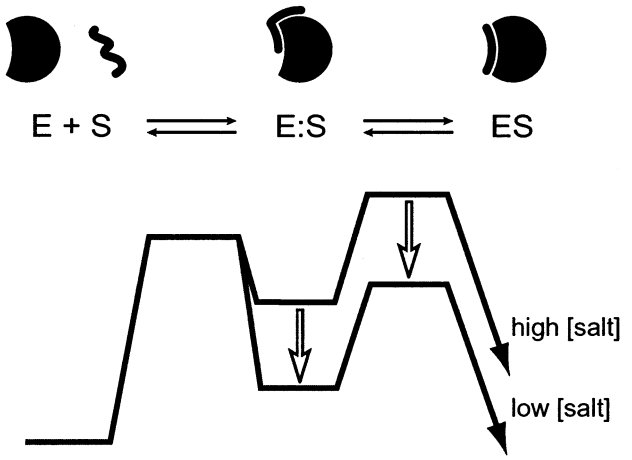

FIGURE 4: Notional mechanism and free energy profile for substrate association by ribonuclease A. The black circle and the solid line represent ribonuclease A and an RNA substrate, respectively. The indentation in the black circle indicates the location of the substrate-binding cleft on ribonuclease A. E:S is an intermediate formed by nonspecific Coulombic interactions. ES is a Michaelis complex formed by specific interactions of the substrate with the substrate-binding cleft. Vertical arrows on the free energy profile indicate the effect of a decrease in salt concentration on the free energy of E:S and the transition state from E:S to ES. At high salt, the formation of ES from E:S determines the rate of substrate association, which is dependent on the salt concentration of the medium. At low salt, the encounter between E and S determines the rate of substrate association, which is independent of the salt concentration.

shown in the salt-rate profile (*21*) and pH-rate profile (Figure 2). The $(k_{cat}/K_M)_{MAX} = 2.8 \times 10^9\ M^{-1}\ s^{-1}$ determined at this low salt concentration is the rate of encounter and the limit of catalysis by RNase A.

Optimization of Catalytic Effectiveness by Ribonuclease A. The significant contribution of physical steps to the overall rate is a distinct characteristic of a perfect enzyme (*2*−*4*). Once the free energy of the transition state of a chemistry step is as low as that of a substrate-association or product-release step, further enhancement of the rate of the chemistry step does not improve overall catalytic efficacy. For such an enzyme, substrate association (or product release) must be improved to the limit allowed by the Haldane relationship (*71*) to maximize catalysis. Accordingly, the evolution of an enzyme to enhance the rate of physical steps is an indication that catalysis of the chemistry step has already been optimized fully.

During catalysis by RNase A, the chemistry step is optimized enough for the substrate-association rate to determine k_{cat}/K_M, at least for a tetranucleotide substrate. Substrate-association proceeds via an intermediate (E:S in Figure 4), most of which proceeds to a Michaelis complex at low salt concentration rather than dissociating to E + S. With longer substrates, the intermediate is dynamic, as RNase A can diffuse in one dimension along a single strand of RNA before forming a Michaelis complex (*70*). Sequence analysis of RNase A homologues from over 40 different vertebrates shows that RNase A is a modern protein that has evolved rapidly (*72*). Despite its nascency, RNase A has the attributes of a perfect catalyst.[7]

[7] This virtue has potential chemotherapeutic utility, as RNase A can serve as a template for the creation of new cytotoxins (*73*).

ACKNOWLEDGMENT

We are grateful to B. R. Kelemen for initiating the use of fluorogenic substrates to study the pH-rate profile of catalysis by RNase A and to W. W. Cleland and D. B. Northrop for numerous contributive discussions.

SUPPORTING INFORMATION AVAILABLE

Data table used to generate Figure 2. This material is available free of charge via the Internet at http://pubs.acs.org.

REFERENCES

1. Wolfenden, R., and Snider, M. J. (2001) The depth of chemical time and the power of enzymes as catalysts, *Acc. Chem. Res. 34*, 938−945.
2. Knowles, J. R., and Albery, W. J. (1977) Perfection in enzyme catalysis: The energetics of triosephosphate isomerase, *Acc. Chem. Res. 10*, 105−111.
3. Albery, W. J., and Knowles, J. R. (1976) Evolution of enzyme function and the development of catalytic efficiency, *Biochemistry 15*, 5631−5640.
4. Burbaum, J. J., Raines, R. T., Albery, W. J., and Knowles, J. R. (1989) Evolutionary optimization of the catalytic effectiveness of an enzyme, *Biochemistry 28*, 9293−9305.
5. Nakatani, H., and Dunford, H. B. (1979) Meaning of diffusion-controlled association rate constants in enzymology, *J. Phys. Chem. 83*, 2662−2665.
6. Berg, O. G., and von Hippel, P. H. (1985) Diffusion-controlled macromolecular interactions, *Annu. Rev. Biophys. Biophys. Chem. 14*, 131−160.
7. Raines, R. T. (1998) Ribonuclease A, *Chem. Rev. 98*, 1045−1066.
8. Thompson, J. E., Venegas, F. D., and Raines, R. T. (1994) Energetics of catalysis by ribonucleases: Fate of the 2′,3′-cyclic intermediate, *Biochemistry 33*, 7408−7414.
9. Thompson, J. E., Kutateladze, T. G., Schuster, M. C., Venegas, F. D., Messmore, J. M., and Raines, R. T. (1995) Limits to catalysis by ribonuclease A, *Bioorg. Chem. 23*, 471−481.
10. McPherson, A., Brayer, G., Cascio, D., and Williams, R. (1986) The mechanism of binding of a polynucleotide chain to pancreatic ribonuclease, *Science 232*, 765−768.
11. Birdsall, D. L., and McPherson, A. (1992) Crystal structure disposition of thymidylic acid tetramer in complex with ribonuclease A, *J. Biol. Chem. 267*, 22230−22236.
12. Fontecilla-Camps, J. C., de Llorens, R., le Du, M. H., and Cuchillo, C. M. (1994) Crystal structure of ribonuclease A·d(ApTpApApG) complex, *J. Biol. Chem. 269*, 21526−21531.
13. Fisher, B. M., Grilley, J. E., and Raines, R. T. (1998) A new remote subsite in ribonuclease A, *J. Biol. Chem. 273*, 34134−34138.
14. Fisher, B. M., Ha, J.-H., and Raines, R. T. (1998) Coulombic forces in protein−RNA interactions: Binding and cleavage by ribonuclease A and variants at Lys7, Arg10, and Lys66, *Biochemistry 37*, 12121−12132.
15. Nogues, M. V., Moussaoui, M., Boix, E., Vilanova, M., Ribo, M., and Cuchillo, C. M. (1998) The contribution of noncatalytic phosphate-binding subsites to the mechanism of bovine pancreatic ribonuclease A, *Cell. Mol. Life Sci. 54*, 766−774.
16. Cuchillo, C. M., Moussaoui, M., Barman, T., Travers, F., and Nogues, M. V. (2002) The exo- or endonucleolytic preference of bovine pancreatic ribonuclease A depends on its subsites' structure and on the substrate size, *Protein Sci. 11*, 117−128.
17. Jensen, D. E., and von Hippel, P. H. (1976) DNA "melting" proteins. I. Effects of bovine pancreatic ribonuclease binding on the conformation and stability of DNA, *J. Biol. Chem. 251*, 7198−7214.
18. Record, M. T., Jr., Lohman, M. L., and De Haseth, P. (1976) Ion effects on ligand−nucleic acid interactions, *J. Mol. Biol. 107*, 145−158.
19. Kelemen, B. R., Klink, T. A., Behlke, M. A., Eubanks, S. R., Leland, P. A., and Raines, R. T. (1999) Hypersensitive substrate for ribonucleases, *Nucleic Acids Res. 27*, 3696−3701.

20. Park, C., Kelemen, B. R., Klink, T. A., Sweeney, R. Y., Behlke, M. A., Eubanks, S. R., and Raines, R. T. (2000) Fast, facile, hypersensitive assays for ribonucleolytic activity, *Methods Enzymol. 341*, 81−94.
21. Park, C., and Raines, R. T. (2001) Quantitative analysis of the effect of salt concentration on enzymatic catalysis, *J. Am. Chem. Soc. 123*, 11472−11479.
22. Alberty, R. A., and Hammes, G. G. (1958) Application of the theory of diffusion-controlled reactions to enzyme kinetics, *J. Phys. Chem. 59*, 154−159.
23. Pörschke, D. (1979) The mode of Mg^{2+} binding to oligonucleotides. Inner sphere complexes as markers for recognition? *Nucleic Acids Res. 6*, 883−898.
24. Pörschke, D. (1978) Thermodynamic and kinetic parameters of oligonucleotide−oligopeptide interactions. Specificity of arginine•inosine association, *Eur. J. Biochem. 86*, 291−299.
25. American Institute of Physics (1972) *American Institute of Physics Handbook*, McGraw-Hill, New York.
26. Tanford, C. (1961) *Physical Chemistry of Macromolecules*, John Wiley & Sons, New York.
27. delCardayré, S. B., Ribo, M., Yokel, E. M., Quirk, D. J., Rutter, W. J., and Raines, R. T. (1995) Engineering ribonuclease A: Production, purification, and characterization of wild-type enzyme and mutants at Gln11, *Protein Eng. 8*, 261−273.
28. Park, C., and Raines, R. T. (2000) Dimer formation by a "monomeric" protein, *Protein Sci. 9*, 2026−2033.
29. Sela, M., Anfinsen, C. B., and Harrington, W. F. (1957) The correlation of ribonuclease activity with specific aspects of tertiary structure, *Biochim. Biophys. Acta 26*, 502−512.
30. Park, C., and Raines, R. T. (2000) Origin of the 'inactivation' of ribonuclease A at low salt concentration, *FEBS Lett. 468*, 199−202.
31. Thompson, J. E., and Raines, R. T. (1995) Value of general acid−base catalysis to ribonuclease A, *J. Am. Chem. Soc. 116*, 5467−5468.
32. Park, C., Schultz, L. W., and Raines, R. T. (2001) Contribution of the active site histidine residues of ribonuclease A to nucleic acid binding, *Biochemistry 40*, 4949−4956.
33. Kelemen, B. R. (1999) Probing ribonuclease A catalysis using nonnatural nucleic acids, Ph.D. Thesis, University of Wisconsin−Madison.
34. Goldberg, J. M., and Baldwin, R. L. (1998) Kinetic mechanism of a partial folding reaction. 1. Properties of the reaction and effects of denaturants, *Biochemistry 37*, 2546−2555.
35. Thompson, J. E. (1995) Catalysis by bovine ribonuclease A−energetics and contributions from the active-site histidines, Ph.D. Thesis, University of Wisconsin−Madison.
36. Quinn, D. M., and Sutton, L. D. (1991) Theoretical basis and mechanistic utility of solvent isotope effects, in *Enzyme Mechanism from Isotope Effects* (Cook, P. F., Ed.) pp 73−126, CRC Press, Boca Raton, FL.
37. Michaelis, L., and Menten, M. L. (1913) Die kinetik der invertinwirkung, *Biochem. Z. 49*, 333−369.
38. Findlay, D., Herries, D. G., Mathias, A. P., Rabin, B. R., and Ross, C. A. (1961) The active site and mechanism of action of bovine pancreatic ribonuclease, *Nature 190*, 781−784.
39. Findlay, D., Herries, D. G., Mathias, A. P., Rabin, B. R., and Ross, C. A. (1962) The active site and mechanism of action of bovine pancreatic ribonuclease. 7. The catalytic mechanism, *Biochem. J. 85*, 152−153.
40. Roberts, G. C. K., Dennis, E. A., Meadows, D. H., Cohen, J. S., and Jardetsky, O. (1969) The mechanism of action of ribonuclease, *Proc. Natl. Acad. Sci. U.S.A. 62*, 1151−1158.
41. Sowa, G. A., Hengge, A. C., and Cleland, W. W. (1997) ^{18}O Isotope effects support a concerted mechanism for ribonuclease A, *J. Am. Chem. Soc. 119*, 2319−2320.
42. Herries, D. G., Mathias, A. P., and Rabin, B. R. (1962) The active site and mechanism of action of bovine pancreatic ribonuclease: 3. The pH-dependence of the kinetic parameters for the hydrolysis of cytidine 2′,3′-phosphate, *Biochem. J. 85*, 127−134.
43. del Rosario, E. J., and Hammes, G. G. (1969) Kinetic and equilibrium studies of the ribonuclease-catalyzed hydrolysis of uridine 2′,3′-cyclic phosphate, *Biochemistry 8*, 1884−1889.
44. Markley, J. L. (1975) Correlation proton magnetic resonance studies at 250 MHz of bovine pancreatic ribonuclease. I. Reinvestigation of the histidine peak assignment, *Biochemistry 14*, 3546−3553.
45. Schultz, L. W., Quirk, D. J., and Raines, R. T. (1998) His···Asp catalytic dyad of ribonuclease A: Structure and function of the wild-type, D121N, and D121A enzymes, *Biochemistry 37*, 8886−8898.
46. Quirk, D. J., and Raines, R. T. (1999) His···Asp catalytic dyad of ribonuclease A: Histidine pK_a values in the wild-type, D121N, and D121A enzymes, *Biophys. J. 76*, 1571−1579.
47. Tipton, K. F., and Dixon, H. B. (1979) Effects of pH on enzymes, *Methods Enzymol. 63*, 183−234.
48. Fisher, B. M., Schultz, L. W., and Raines, R. T. (1998) Coulombic effects of remote subsites on the active site of ribonuclease A, *Biochemistry 37*, 17386−17401.
49. Knowles, J. R. (1976) The intrinsic pK_a values of functional groups in enzymes: Improper deductions from the pH-dependence of steady-state parameters, *CRC Crit. Rev. Biochem. 4*, 165−173.
50. Brocklehurst, K. (1994) A sound basis for pH-dependent kinetic studies on enzymes, *Protein Eng. 7*, 291−299.
51. Witzel, H. (1963) The function of the pyrimidine base in the ribonuclease reaction, *Prog. Nucleic Acid Res. 2*, 221−258.
52. Eftink, M. R., and Biltonen, R. L. (1983) Energetics of ribonuclease A catalysis. 1. pH, ionic strength, and solvent isotope dependence of the hydrolysis of cytidine cyclic 2′,3′-phosphate, *Biochemistry 22*, 5123−5134.
53. Cleland, W. W. (1977) Determining the chemical mechanisms of enzyme-catalyzed reactions by kinetic studies, *Adv. Enzymol. Relat. Areas Mol. Biol. 45*, 273−387.
54. Alberty, R. A., and Bloomfield, V. (1963) Multiple intermediates in steady-state enzyme kinetics, *J. Biol. Chem. 238*, 2804−2810.
55. Cleland, W. W. (1986) Enzyme kinetics as a tool for determination of enzyme mechanisms, in *Investigations of Rates and Mechanisms of Reactions* (Bernasconi, C. F., Ed.) pp 791−870, John Wiley & Sons, New York.
56. Matta, M. S., and Vo, D. T. (1986) Proton inventory of the second step of ribonuclease catalysis, *J. Am. Chem. Soc. 108*, 5316−5318.
57. Schowen, R. L. (1977) Solvent isotope effects on enzymic reactions, in *Isotope Effects on Enzyme-Catalyzed Reactions* (Cleland, W. W., O'Leary, M. H., and Northrop, D. B., Eds.) pp 64−99, University Park Press, Baltimore.
58. Karsten, W. E., Lai, C.-J., and Cook, P. F. (1995) Inverse solvent isotope effects in the NAD-malic enzyme reaction are the result of the viscosity difference between D_2O and H_2O: Implications for solvent isotope effect studies, *J. Am. Chem. Soc. 117*, 5914−5918.
59. Kramers, H. A. (1940) Brownian motion in a field of force and the diffusion model of chemical reactions, *Physica (Amsterdam) 7*, 284−304.
60. Blacklow, S. C., Raines, R. T., Lim, W. A., Zamore, P. D., and Knowles, J. R. (1988) Triosephosphate isomerase catalysis is diffusion controlled, *Biochemistry 27*, 1158−1167.
61. Messmore, J. M., Fuchs, D. N., and Raines, R. T. (1995) Ribonuclease A: Revealing structure−function relationships with semisynthesis, *J. Am. Chem. Soc. 117*, 8057−8060.
62. Lohman, T. M. (1986) Kinetics of protein−nucleic acid interactions: Use of salt effects to probe mechanisms of interaction, *CRC Crit. Rev. Biochem. 19*, 191−245.
63. Sharp, K., Fine, R., and Honig, B. (1987) Computer simulations of the diffusion of a substrate to an active site of an enzyme, *Science 236*, 1460−1463.
64. Getzoff, E. D., Cabelli, D. E., Fisher, C. L., Parge, H. E., Viezzoli, M. S., Banci, L., and Hallewell, R. A. (1992) Faster superoxide dismutase mutants designed by enhancing electrostatic guidance, *Nature 358*, 347−351.
65. Wade, R. C., Gabdoulline, R. R., Ludemann, S. K., and Lounnas, V. (1998) Electrostatic steering and ionic tethering in enzyme-ligand binding: Insights from simulations, *Proc. Natl. Acad. Sci. U.S.A. 95*, 5942−5949.
66. Sinha, N., and Smith-Gill, S. J. (2002) Electrostatics in protein binding and function, *Curr. Protein Pept. Sci. 3*, 601−614.
67. Chou, K.-C., and Zhou, G.-P. (1982) Role of the protein outside active site on the diffusion-controlled reaction of enzyme, *J. Am. Chem. Soc. 104*, 1409−1413.

68. Northrup, S. H., Boles, J. O., and Reynolds, J. C. (1988) Brownian dynamics of cytochrome *c* and cytochrome *c* peroxidase association, *Science 241*, 67−70.

69. von Hippel, P. H., and Berg, O. G. (1989) Facilitated target location in biological systems, *J. Biol. Chem. 264*, 675−678.

70. Kelemen, B. R., and Raines, R. T. (1999) Extending the limits to enzymatic catalysis: Diffusion of ribonuclease A in one dimension, *Biochemistry 38*, 5302−5307.

71. Haldane, J. B. S. (1930) *Enzymes*, pp 80−83, Longmans, Green and Company, London, UK.

72. Beintema, J. J., Schüller, C., Irie, M., and Carsana, A. (1988) Molecular evolution of the ribonuclease superfamily, *Prog. Biophys. Mol. Biol. 51*, 165−192.

73. Leland, P. A., and Raines, R. T. (2001) Cancer chemotherapy—ribonucleases to the rescue, *Chem. Biol. 8*, 405−413.

BI026076K